

Transitions between inherent structures in water

Nicolas Giovambattista,¹ Francis W. Starr,² Francesco Sciortino,³ Sergey V. Buldyrev,¹
and H. Eugene Stanley¹

¹*Center for Polymer Studies and Department of Physics, Boston University, Boston, Massachusetts 02215*

²*Polymers Division and Center for Theoretical and Computational Materials Science, National Institute of Standards and Technology, Gaithersburg, Maryland, 20899*

³*Dipartimento di Fisica, Istituto Nazionale per la Fisica della Materia, and INFN Center for Statistical Mechanics and Complexity, Università di Roma La Sapienza, Piazza le A. Moro 2, I-00185 Roma, Italy*

(Received 24 August 2001; published 18 March 2002)

The energy landscape approach has been useful to help understand the dynamic properties of supercooled liquids and the connection between these properties and thermodynamics. The analysis in numerical models of the inherent structure (IS) trajectories—the set of local minima visited by the liquid—offers the possibility of filtering out the vibrational component of the motion of the system on the potential energy surface and thereby resolving the slow structural component more efficiently. Here we report an analysis of an IS trajectory for a widely studied water model, focusing on the changes in hydrogen bond connectivity that give rise to many IS's separated by relatively small energy barriers. We find that while the system *travels* through these IS's, the structure of the bond network is continuously modified, exchanging linear bonds for bifurcated bonds and usually reversing the exchange to return to nearly the same initial configuration. For the 216-molecule system we investigate, the time scale of these transitions is as small as the simulation time scale (≈ 1 fs). Hence, for water, the transition between each of these IS's is relatively small and eventual relaxation of the system occurs only by many of these transitions. We find that during IS changes the molecules with the greatest displacements move in small “clusters” of 1–10 molecules with displacements of ≈ 0.02 – 0.2 nm, not unlike simpler liquids. However, for water these clusters appear to be somewhat more branched than the linear “stringlike” clusters formed in a supercooled Lennard-Jones system found by Glotzer and her collaborators.

DOI: 10.1103/PhysRevE.65.041502

PACS number(s): 61.43.Fs, 61.20.Ne

I. INTRODUCTION

It is believed that the properties of liquids can be understood as motion of the system in a high-dimensional complex potential energy surface (PES) [1–6]. As a liquid is cooled toward the glassy state, the system is increasingly found near local potential energy minima, called inherent structure (IS) configurations [2]. As the temperature decreases, the description of the dynamics in terms of motion on the PES becomes increasingly appropriate. In this description, in the glassy state, the system is localized in one of the potential energy basins [7–10].

While such a picture of liquid dynamics is difficult to verify experimentally, computer simulation offers an excellent opportunity to explore these ideas. For a predefined liquid potential, a liquid trajectory can be generated via molecular dynamics simulation and the local potential energy minima can be evaluated by an energy minimization method [2]. With this procedure, the motion in phase space is converted into a minimum-to-minimum trajectory, or *IS trajectory*. A general picture of the system moving among a set of basins surrounding the multitude of local minima has evolved. More specifically, simulations have shown that both the depth of the minima sampled by the system, and the number of these minima decrease on cooling [5,10,11]. Simulations have also shown that, below a crossover temperature T_{\times} , only rare fluctuations bring the system to a saddle point and hence activated processes become important for relaxation of the liquid [7,9,12–14]. For the system we study, T_{\times} coincides numerically [9,14–17] with the critical

temperature identified by mode coupling theory (MCT), which has been widely used to understand the dynamics of liquids on “weak” supercooling (the T range where characteristic relaxation times approach $\approx 10^{-8}$ s) [18].

The description of the real motion of the system as an IS trajectory becomes a powerful way of separating the vibrational contribution, responsible for the thermal broadening of instantaneous measurements, from the slow structural component [19]. Such an approach becomes even more powerful below T_{\times} , since most of the instantaneous configurations are far from saddles, making correlation functions calculated from the IS trajectory able to fully account for the α -relaxation dynamics [7].

Here we study the IS trajectory below T_{\times} for the extended simple point charge (SPC/E) potential [20], a well-studied model for water. The dynamics of the SPC/E model have been shown to be consistent with the predictions of MCT [21,22]. Additionally, the PES of the SPC/E model has been studied in detail above T_{\times} and a thermodynamic description of the supercooled states based on the PES has been presented [11,23]. Here we focus on the geometrical properties of the motion, once the vibrational component is subtracted. The possibility of performing such a study below T_{\times} , with a very fine time coarse graining, allows us to examine the structural changes that accompany the basin transitions and to describe an elementary step of the diffusive process in terms of hydrogen-bond network rearrangement.

This work is organized as follows. In Sec. II we provide the simulation details. In Sec. III we analyze the displacement of the molecules in these IS transitions and in Sec. IV

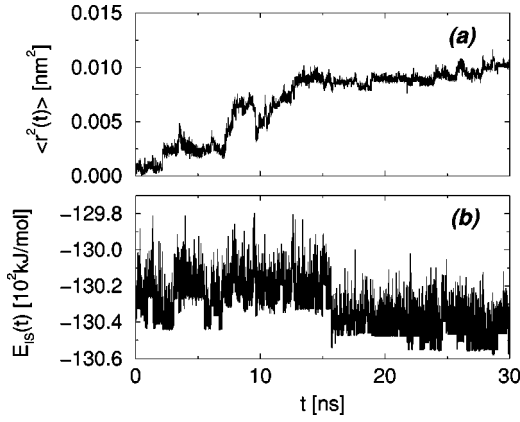


FIG. 1. (a) Mean square displacement and (b) IS energy for the inherent structures as a function of time for the studied 216-molecule system. The time interval between adjacent IS's in both figures is 1 ps. While it is possible to track IS's transitions from the potential energy, this is not the case for the mean square displacement. Note that the amplitude of the peaks of the potential energy is $\approx 10\text{--}20$ kJ/mol, the same order of magnitude as a HB energy.

we study the corresponding changes in the hydrogen-bond (HB) network. Finally, in Sec. V we present a brief summary.

II. SIMULATION

Our results are based on molecular dynamics simulations of the SPC/E model [20] of water for 216 molecules, at fixed density $\rho = 1$ g/cm³. The numerical procedure is described in Ref. [22]. The integration time step δt is 2 fs. The mode coupling temperature for this density is $T_{MCT} \approx 194$ K [22]. We analyze trajectories at $T = 180$ K, so that the system is in the deep supercooled liquid state. At this temperature, the diffusion coefficient is more than four orders of magnitude smaller than its value at $T = 300$ K and only a few molecules move significantly (with displacements larger than 0.025 nm) at each simulation time step [24]. Our system is started from equilibrated configurations at 190 K, which relax for nearly 920 ns at 180 K before we record and analyze the trajectory. At such a low temperature, a slow aging in the trajectory could be present; however, the aging should not affect the qualitative picture we present.

We have generated one trajectory of 30 ns, sampling configurations at each 1 ps. For each configuration we find the corresponding IS using conjugate gradient minimization. In this way, we obtain 30 000 configurations with the corresponding IS. Since we could miss some IS transitions with 1 ps sampling, we also ran four independent 20 ps simulations sampling the IS at 4 fs. In this way, we obtain another 20 000 configurations with the corresponding IS's.

III. INHERENT STRUCTURE TRAJECTORIES

Figure 1 shows an example of the potential energy of the IS, $E_{IS}(t)$, and the mean square displacement of the oxygen atoms $\langle r^2(t) \rangle$ starting from a single arbitrary starting time. At $T = 180$ K, the slowest collective relaxation time τ_α

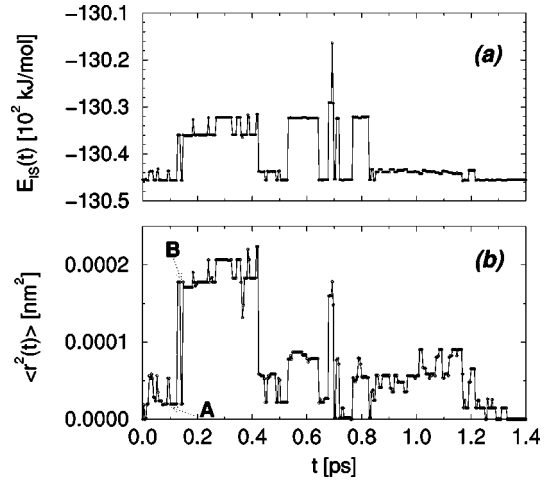


FIG. 2. (a) IS energy and (b) mean square displacement for the IS's obtained using a sampling interval of 4 fs, twice the simulation time step. The correlation between E_{IS} and $\langle r^2(t) \rangle$ is evident. Also, we see that it is necessary to sample the IS's with a mesh of the order of the simulation time step to detect all the IS's visited by the system.

>200 ns [22]. The IS trajectory in Fig. 1 has a mesh of 1 ps and covers a total time of 30 ns. In this time interval, $\langle r^2(t) \rangle$ is about 1 \AA^2 , i.e., much less than the corresponding value of the average nearest neighbor distance of 2.8 \AA . Figure 2 shows an enlargement of the IS trajectory using a much smaller time mesh (4 fs, twice the simulation time step). Figure 2 shows that changes occur via discrete transitions, with an average duration of ≈ 0.2 ps. The transitions are characterized by an energy change of $\approx 10\text{--}20$ kJ/mol and an oxygen atom square displacement of the order of 0.01 \AA^2 ; they appear to constitute the elementary step underlying the diffusional process in the system.

We note that it is impossible to identify the transition unless the quenching time step is of the order of the simulation time step. This is in distinct contrast to a Lennard-Jones liquid, where such small continuous changes are not present [7]. The difference, we will show, is attributable to the hydrogen bonds. This time scale for IS transitions is in accord with other work on the TIP2S water model, at $T = 298$ K [19].

In Fig. 2, we see that sharp changes in $E_{IS}(t)$ coincide with the sharp changes in $\langle r^2(t) \rangle$. This confirms that the system is repeatedly visiting specific configurations, since $\langle r^2(t) \rangle$ and $E_{IS}(t)$ take on discrete values. The results shown in Fig. 2 imply that the system often returns to the original basin because both the difference in energy and the displacement approach zero at the end of the time interval.

To aid in understanding the distribution of the displacements during the IS changes [such as those between the two IS's labeled A and B in Fig. 2(b)], Fig. 3 shows the displacements u of all 216 individual molecules from IS A to IS B. We see that there is a relatively small set of molecules with a large displacement. A snapshot of the eight molecules with the largest displacement is shown in Fig. 4. Interestingly, we find that this set of molecules forms a cluster of bonded

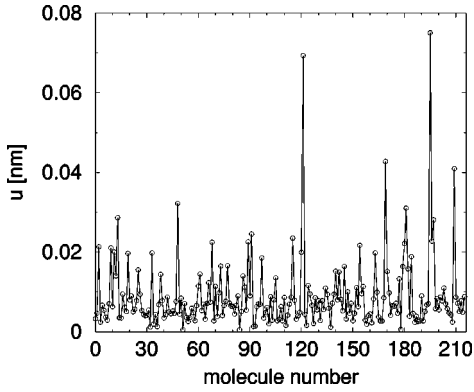


FIG. 3. Displacement of each molecule in the transition from IS A to IS B shown in Fig. 2(b).

molecules. Indeed, for all cases studied, we found that the set of molecules which are most displaced form a cluster of bonded molecules. The observed clustering phenomenon characterizes the IS transitions in water and can be interpreted as the analog of the stringlike motion observed in simple atomistic liquids [7] and connected to the presence of dynamical heterogeneities [25]. Similar results were found by Ohmine *et al.* using the TIP4P and TIPS2 models for water [26].

To characterize the distribution of individual molecular displacements between different IS's more carefully, we show the distribution of displacements u of the oxygen atoms $P(u, \delta t = 4 \text{ fs})$ in Fig. 5. The time difference δt is twice the integration time step [27]. We collected data from all transitions in four independent 20 ps trajectories for the results reported in Fig. 5. Note that $P(u)$ was previously studied by Schröder *et al.* for a binary Lennard-Jones (LJ) mixture [7].

We find that the distribution of displacements is monotonic and does not allow us to detect a characteristic length

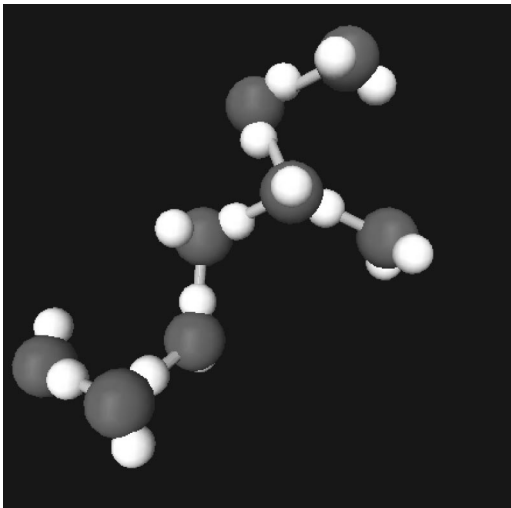


FIG. 4. Snapshot of the system in the IS labeled A in Fig. 2(b). Only the eight molecules with displacement larger than 0.025 nm are shown here. Hydrogen-bonded molecules are connected by tubes. Note that all eight molecules are nearby and form a cluster, which unlike the LJ case, is bonded and less stringlike.

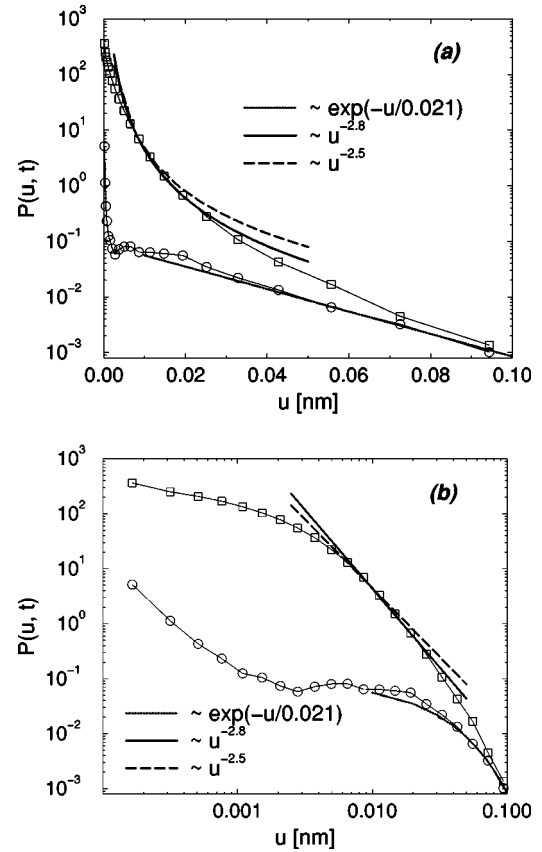


FIG. 5. Distribution of displacements u of the oxygen atoms between IS changes, $P(u, t)$, evaluated at $t = 4 \text{ fs}$. We show the distribution of all the displacements of the molecules (squares) and the distribution for the largest displacement in an IS transition (circles). For comparison, we divided the largest displacement distribution by the number of molecules. We present both (a) linear-log and (b) log-log graphs to show the power-law behavior for $u \approx 0.01 \text{ nm}$ and the exponential tail of the distributions. We also show the prediction of elasticity theory $P(u) \sim u^{-2.5}$.

which could help in distinguishing between diffusive and nondiffusive basin changes. $P(u, t)$ for $t = \delta t$ shows an apparent power law with a negative slope of about -2.8 ± 0.2 , followed by an exponential tail. To highlight the exponential tail, we present the data in a linear-log plot Fig. 5(a), showing that the tail in $P(u, \delta t = 4 \text{ fs})$ is mostly due to these highly “mobile molecules.” The characteristic length of the exponential tail is 0.2 \AA , about 15 times smaller than the nearest neighbor oxygen distance of 2.8 \AA and in agreement with the finding of Schröder *et al.* for the LJ case, where the characteristic length was about 1/8 of the nearest neighbor distance.

Schröder *et al.* interpreted the power-law contribution to $P(u, \delta t)$ as a response of the system to the diffusing molecules. In elasticity theory [28], a local displacement at the origin produces a distribution of displacements which scales with the distance R from the origin as R^{-2} . Hence the distribution of displacements u scales as $u^{-2.5}$ [28]. In contrast with the LJ case, the exponent we find is slightly larger than 2.5, a discrepancy that may be related to the application of a

continuum theory at a length scale where molecular details are still relevant. In the spirit of elasticity theory, the deviation of the distribution at small u values from the power law arises from the cutoff introduced by the finite size of the simulation. Indeed, small u values are produced at large R and hence are missing in a finite simulation box.

Although a subset of “highly mobile” molecules is identifiable using a predefined threshold value in a single basin change, there is no unambiguous general criterion for identifying the molecules responsible for a single basin transition.

An important open question is the relation between the displacement distribution functions for $t = \delta t$ (Fig. 5) and the same distribution evaluated for an arbitrary time interval t . A full knowledge of this relation may shed light on the elementary stochastic process that best describes the dynamics of the deep supercooled state. This calculation requires a significant computational investment due to the very large number of IS configurations that need to be evaluated. Despite such difficulties, it is a promising research line for the near future.

IV. HB NETWORK RESTRUCTURING

Liquid water is an interesting system for studying the physical processes that accompany basin transitions. The unusual dynamic and thermodynamic properties of water are believed to be connected to the microscopic behavior of hydrogen bonding. Many experiments suggest that this tetrahedral HB network has defects, such as an extra (fifth) molecule in the first coordination shell [29,30]. Indeed, such five-coordinated molecules have been directly identified in simulations and the defects were found to be a catalyst for motion in the system [31], making an obvious possible connection between network defects promoting diffusion and the basin transitions that give rise to diffusive motion of that system.

To obtain a physical picture of the IS transitions for water and hopefully to better understand the source of these transitions, we focus on the small changes in the HB network along a minimum-to-minimum trajectory. Analysis of the HB network based on IS configurations has shown that local PES minima are characterized by both linear bonds (LB’s) and bifurcated bonds (BB’s) [31] whose fraction is both temperature and density dependent. The HB network tends toward a perfect random tetrahedral network on cooling, or on lowering the pressure [23]. Here we emphasize the changes in the network associated with IS transitions.

To quantify the bonding changes, it is necessary to employ an arbitrary bond definition. Previous work has indicated that several definitions provide physically reasonable results. Here we use the definition that two molecules are bonded if their oxygen-oxygen distance is less than 3.5 Å and their mutual potential energy is negative [31]. Using this definition, we obtain the equilibrium distribution of the potential energy for the LB’s and BB’s, shown in Fig. 6.

These results agree with previous findings, based on different models [32–34]. The distribution of BB energies is bimodal with peaks at roughly -6 kJ/mol or

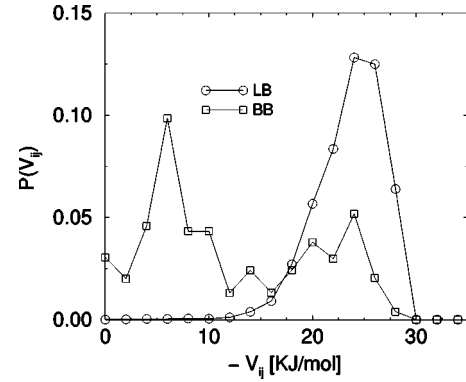


FIG. 6. Distribution function for the pair interaction energy V_{ij} for the LB’s and BB’s in the IS. Note the bimodal distribution for BB’s and unimodal distribution for LB’s.

-22.5 kJ/mol, while the LB energy distribution is unimodal with a peak at roughly -24 kJ/mol. Therefore, the energy associated with a change in the HB network due to losing *one* LB and creating *two* BB’s ranges roughly from -21 kJ/mol to 12 kJ/mol, depending on which of the two possible BB’s are created. The relative intensities of the peaks of the BB energy distribution suggest that such a mechanism would more likely lead to an increase in the overall energy. A comparison of the HB energy changes with those found in Fig. 1 suggests that interchanges between LB’s and BB’s can explain the existence of a multitude of IS’s separated by very small energy barriers. More specifically, we hypothesize that changes increasing E_{IS} found in Fig. 1 are due to processes LB \rightarrow BB, while changes decreasing E_{IS} are due to the processes BB \rightarrow LB. To confirm or reject this hypothesis, we study the distributions of LB’s and BB’s for IS’s just before and just after positive and negative “jumps” in the potential energy [Fig. 1(b)] with energy larger than 9 kJ/mol [35]. These IS’s are schematically shown in Fig. 7(a). The corresponding distributions for LB’s and BB’s are shown in Fig. 7(b) and 7(c). We see that during PE increases, the average number of LB’s decreases while the number of BB’s increases; the opposite situation occurs when the potential energy decreases. The distribution for BB’s has peaks at even numbers of BB’s, which we expect since for each LB lost, two BB’s appear, also implying that the distribution should be zero for odd numbers of BB’s [36]. The anticorrelation of the BB and LB changes is a strong indicator that a mechanism whereby the system accesses higher-energy states is via LB \rightarrow BB transitions.

To reinforce the hypothesis that the basin change is associated with a restructuring of the local connectivity, Fig. 8 shows the number of molecules with a coordination number equal to 3, 4, or 5 as a function of time for a characteristic time interval and contrasts these data with the time dependence of $\langle r^2(t) \rangle$. A clear anticorrelation is observed between the time dependence of the number of threefold- and fivefold-coordinated molecules compared to the time dependence of the fourfold-coordinated molecules, supporting the proposed interchange mechanism. The fact that increases in the fraction of BB’s coincide with changes in $\langle r^2(t) \rangle$ sup-

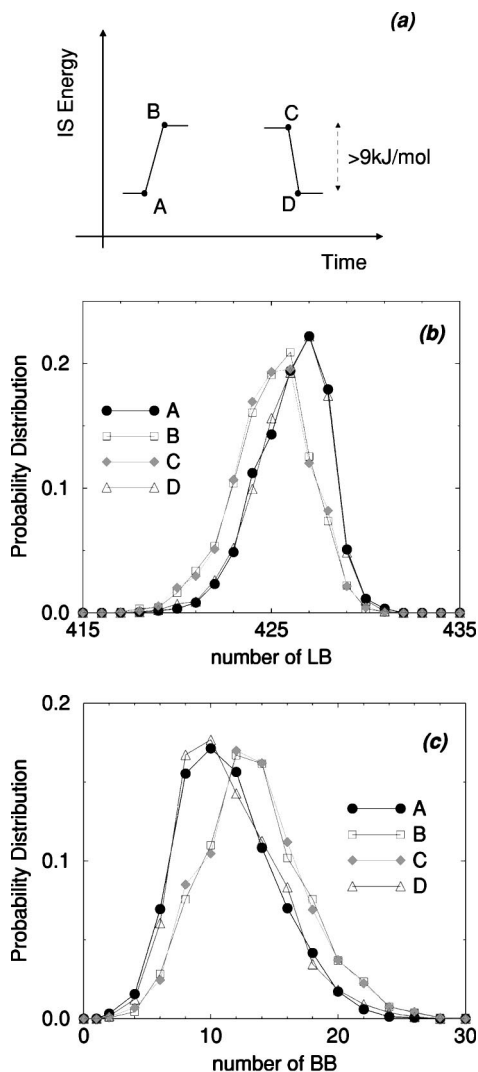


FIG. 7. (a) shows schematically the separation of IS's used to measure the probability distributions for (b) LB's and (c) BB's. Circles correspond to the distribution calculated over the IS just before an increase in potential energy larger than 9 kJ/mol, i.e. when the system is in IS A shown in (a). Squares correspond to the distribution calculated over the IS just after an increase in potential energy larger than 9 kJ/mol, i.e., when the system is in IS B shown in (a). Similarly, diamonds correspond to the distribution calculated over the IS just before a decrease in potential energy larger than 9 kJ/mol, when the system is in IS C shown in (a). Triangles correspond to the distribution calculated over the IS just after a decrease in potential energy larger than 9 kJ/mol, when the system is in IS D shown in (a).

ports the expectation that motion is a result of network imperfections.

V. SUMMARY

We have presented a detailed analysis of the motion on the PES of a 216-water-molecule system interacting via the SPC/E potential in a deeply supercooled state, below the MCT temperature. At this temperature, the system populates

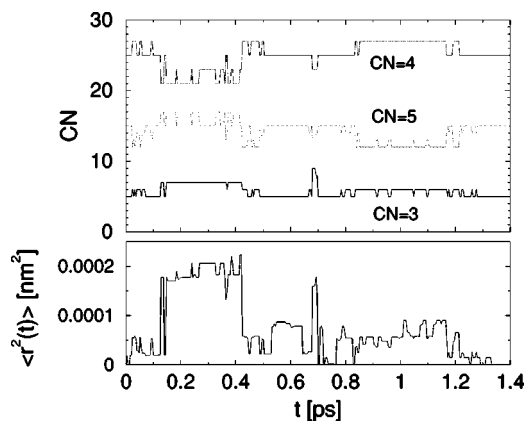


FIG. 8. Number of molecules with coordination number (CN) of 3, 4, and 5 versus time, for the IS's corresponding to Fig. 2. The plot for a CN of 4 is shifted down by 400 units for better comparison. Also shown is $\langle r^2(t) \rangle$. We see how the tetrahedral network acquires both types of defect (CN equals 3 and 5) while the system explores different IS's.

basins of local minima. In these conditions, the analysis of the IS trajectories provides a very clean description of the slow α -relaxation process, filtering nearly all vibrational motions.

We have shown that an inherent structure transition is observed about every 0.2 ps. It is the collection of these numerous small transitions that gives rise to the structural relaxation of the system. These fast transitions are characterized by a broad distribution of individual molecule displacements, without a clear characteristic length. Future work must address the issue of the prediction of $P(u, t)$ from the knowledge of $P(u, \delta t)$.

We perform an analysis of the geometry of the individual event and find that the most mobile molecules are clustered. The analysis of the changes in HB connectivity associated with IS changes reveals that these transitions are associated with the breaking and reformation of HB's. This result is in accord with the work of Ohmine and colleagues [19,26] for TIP4P. We have shown that the transitions associated with an increase in the energy correspond to the breaking of linear bonds and to the simultaneous formation of bifurcated bonds. Similarly, the transitions associated with a decrease in the energy correspond to the breaking of bifurcated bonds and to the simultaneous formation of linear bonds.

This result supports the hypothesis that the linear to bifurcated transition can be considered as an elementary step in the rearrangement of the HB network.

ACKNOWLEDGMENTS

We thank T.B. Schröder, S. Sastry, and S.C. Glotzer for interesting discussions. N.G. wants to thank I. Ohmine for fruitful discussions and suggestions. F.S. acknowledges support from INFN-PRA-HOP and Iniziative Calcolo Parallelo and MURST COFIN2000. This work was supported by the NSF Chemistry Program.

- [1] M. Goldstein, *J. Chem. Phys.* **51**, 3728 (1969).
- [2] F.H. Stillinger and T.A. Weber, *Phys. Rev. A* **28**, 2408 (1983).
- [3] F.H. Stillinger, *Science* **267**, 1935 (1995).
- [4] C.A. Angell, *Science* **267**, 1924 (1995).
- [5] S. Sastry, P.G. Debenedetti, and F.H. Stillinger, *Nature (London)* **393**, 554 (1998).
- [6] P.G. Debenedetti and F.H. Stillinger, *Nature (London)* **410**, 259 (2001).
- [7] T.B. Schröder, S. Sastry, J.C. Dyre, and S.C. Glotzer, *J. Chem. Phys.* **112**, 9834 (2000).
- [8] A. Heuer, *Phys. Rev. Lett.* **78**, 4051 (1997); S. Buchner and A. Heuer, *Phys. Rev. E* **60**, 6507 (1999).
- [9] L. Angelani, G. Parisi, G. Ruocco, and G. Viliani, *Phys. Rev. Lett.* **81**, 4648 (1998).
- [10] F. Sciortino, W. Kob, and P. Tartaglia, *Phys. Rev. Lett.* **83**, 3214 (1999).
- [11] A. Scala, F.W. Starr, E. La Nave, F. Sciortino, and H.E. Stanley, *Nature (London)* **406**, 166 (2000).
- [12] J.P.K. Doye and D. Wales, *Phys. Rev. Lett.* **86**, 5719 (2001).
- [13] T. Keyes, *J. Phys. Chem. A* **101**, 2921 (1997).
- [14] E. La Nave, A. Scala, F.W. Starr, F. Sciortino, and H.E. Stanley, *Phys. Rev. Lett.* **84**, 4605 (2000); E. La Nave, A. Scala, F.W. Starr, H.E. Stanley, and F. Sciortino, *Phys. Rev. E* **64**, 036102 (2001).
- [15] F. Sciortino and P. Tartaglia, *Phys. Rev. Lett.* **78**, 2385 (1997).
- [16] C. Donati, F. Sciortino, and P. Tartaglia, *Phys. Rev. Lett.* **85**, 1464 (2000).
- [17] E. La Nave, F. Sciortino, and H.E. Stanley, *Phys. Rev. Lett.* **88**, 035501 (2002).
- [18] W. Götze and L. Sjøgren, *Rep. Prog. Phys.* **55**, 241 (1992).
- [19] I. Ohmine and H. Tanaka, *Chem. Rev.* **93**, 2545 (1993), and references therein.
- [20] H.J. Berendsen, J.R. Grigera, and T.P. Stroatsma, *J. Phys. Chem.* **91**, 6269 (1987).
- [21] F. Sciortino, P. Gallo, P. Tartaglia, and S-H. Chen, *Phys. Rev. E* **54**, 6331 (1996); P. Gallo, F. Sciortino, P. Tartaglia, and S.H. Chen *Phys. Rev. Lett.* **76**, 2730 (1996); F. Sciortino, L. Fabbian, S-H. Chen, and P. Tartaglia, *Phys. Rev. E* **56**, 5397 (1997); L. Fabbian, A. Latz, R. Schilling, F. Sciortino, P. Tartaglia, and C. Theis, *ibid.* **60**, 5768 (1999); **62**, 2388 (2000); C. Theis, A. Latz, R. Schilling, F. Sciortino, and P. Tartaglia *ibid.* **62**, 1856 (2000).
- [22] F.W. Starr, F. Sciortino, and H.E. Stanley, *Phys. Rev. E* **60**, 6757 (1999).
- [23] F.W. Starr, S. Sastry, E. La Nave, A. Scala, H.E. Stanley, and F. Sciortino, *Phys. Rev. E* **63**, 041201 (2001).
- [24] The Adam and Gibbs hypothesis G. Adam and J.H. Gibbs, *J. Chem. Phys.* **43**, 139 (1965) states that flow in a supercooled fluid involves cooperative motion of molecules. For recent experimental work on cooperative motions see M.T. Cicerone, F.R. Blackburn, and M.D. Ediger, *J. Chem. Phys.* **102**, 471 (1995); E.R. Weeks, J.C. Crocker, A.C. Levitt, A. Schofield, and D.A. Weitz, *Science* **287**, 627 (2000); K. Schmidt-Rohr and H.W. Spiess, *Phys. Rev. Lett.* **66**, 3020 (1991); A. Heuer, M. Wilhelm, H. Zimmermann, and H.W. Spiess, *ibid.* **75**, 2851 (1995).
- [25] M. Hurley and P. Harrowell, *Phys. Rev. E* **52**, 1694 (1995); W. Kob, C. Donati, S.J. Plimpton, P.H. Poole, and S.C. Glotzer, *Phys. Rev. Lett.* **79**, 2827 (1997); C. Donati, J.F. Douglas, W. Kob, S.J. Plimpton, P.H. Poole, and S.C. Glotzer, *ibid.* **80**, 2338 (1998); B. Doliwa and A. Heuer, *ibid.* **80**, 4915 (1998).
- [26] M. Matsumoto and I. Ohmine, *J. Chem. Phys.* **104**, 2705 (1996); I. Ohmine and S. Saito, *Acc. Chem. Res.* **32**, 741 (1999), and references therein.
- [27] If during the time interval δt the system does not change IS, the contribution to $P(u, \delta t)$ appears only for $u=0$ and hence does not modify the shape of the distribution.
- [28] J.C. Dyre, *Phys. Rev. E* **59**, 2458 (1999); **59**, 7243 (1999).
- [29] *Hydrogen Bonded Liquids*, edited by J. Dore and J. Teixeira (Kluwer, Dordrecht, 1991), pp. 171–183.
- [30] E. Grünwald, *J. Am. Chem. Soc.* **108**, 5719 (1986); A.H. Narten and H.A. Levy, *Science* **165**, 447 (1969); P.A. Giguere, *J. Chem. Phys.* **87**, 4835 (1987); G.E. Walrafen, M.S. Hokmabadi, W.H. Yang, Y.C. Chu, and B. Monosmith, *J. Phys. Chem.* **93**, 2909 (1989).
- [31] F. Sciortino, A. Geiger, and H.E. Stanley, *Phys. Rev. Lett.* **65**, 3452 (1990); *Nature (London)* **354**, 218 (1991); *J. Chem. Phys.* **96**, 3857 (1992).
- [32] F.H. Stillinger and A. Rahman, *J. Chem. Phys.* **60**, 1545 (1974).
- [33] H. J. C. Berendsen, J. C. M. Postma, W. F. Von Gunsteren, and J. Hermans in *Intermolecular Forces*, edited by B. Pullman (Reidel, Dordrecht, 1981), p. 331.
- [34] W.L. Jorgensen, J. Chandrasekhar, J.D. Madura, R.W. Impey, and M.L. Klein, *J. Chem. Phys.* **79**, 926 (1983).
- [35] We found from Fig. 1 that most of the “jumps” in potential energy correspond to changes in $|E_{IS}|$ larger than 9 kJ/mol. We found similar results for a lower cutoff in energy of 1 kJ/mol.
- [36] We found that the distribution is not exactly zero for odd numbers of BB’s, which is a consequence of the bond definition. Using the definition that two molecules are bonded if their oxygen-oxygen distance is less than 0.35 nm and their interaction energy is less than a fixed value $E_{HB}=0$, we found that there exist a few cases in which one hydrogen atom is “shared” by three oxygens (instead of two as in the case of a BB). We tried different values for E_{HB} and found that these “trifurcated” bonds (TB’s) disappear if E_{HB} is reduced to -10 kJ/mol. These TB’s can also contribute to the presence of an even number of BB’s appearing in the distribution. The ratio of BB’s to TB’s for $E_{HB}=0$ and -5 kJ/mol is 20:1 and 24:1. We also checked that the distribution for BB’s at $E_{HB} = -10$ kJ/mol is zero for odd numbers of molecules.